Electronic Supplementary Material (ESI) for Journal of Materials Chemistry A.

$M_xCo_{3-x}O_4$(M = Co, Mn, Fe) Porous Nanocages Derived from Metal–Organic Frameworks as Efficient Water Oxidation Catalysts

Jie Wei,[a] Yingying Feng,[a] Yan Liu,[a] and Yong Ding[ab]*

[a] State Key Laboratory of Applied Organic Chemistry, Key Laboratory of Nonferrous Metal Chemistry and Resources Utilization of Gansu Province, College of Chemistry and Chemical Engineering, Lanzhou University,
Lanzhou 730000, China. Email: dingyong1@lzu.edu.cn

[b] State Key Laboratory for Oxo Synthesis and Selective Oxidation, Lanzhou Institute of Chemical Physics, Chinese Academy of Sciences, Lanzhou 730000, China

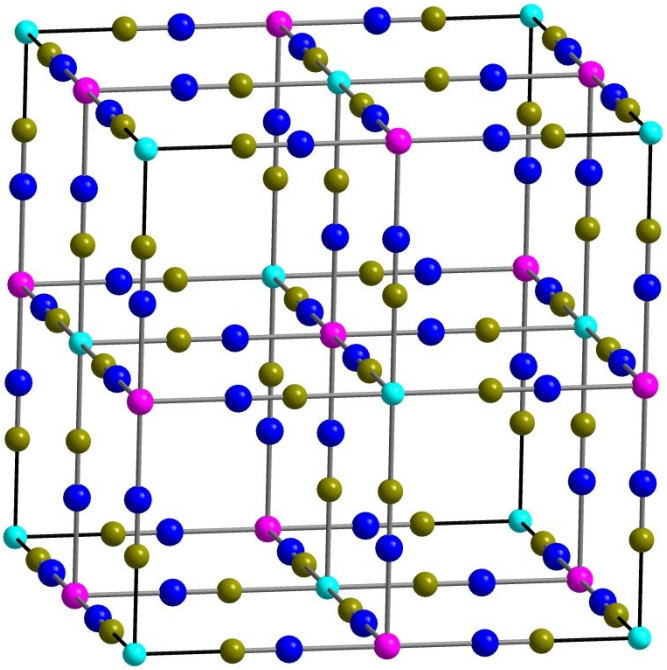

Figure S1. Representation of a cubic Prussian blue-type structure (transition metal, turquoise/pink; C, dark yellow; N, blue).

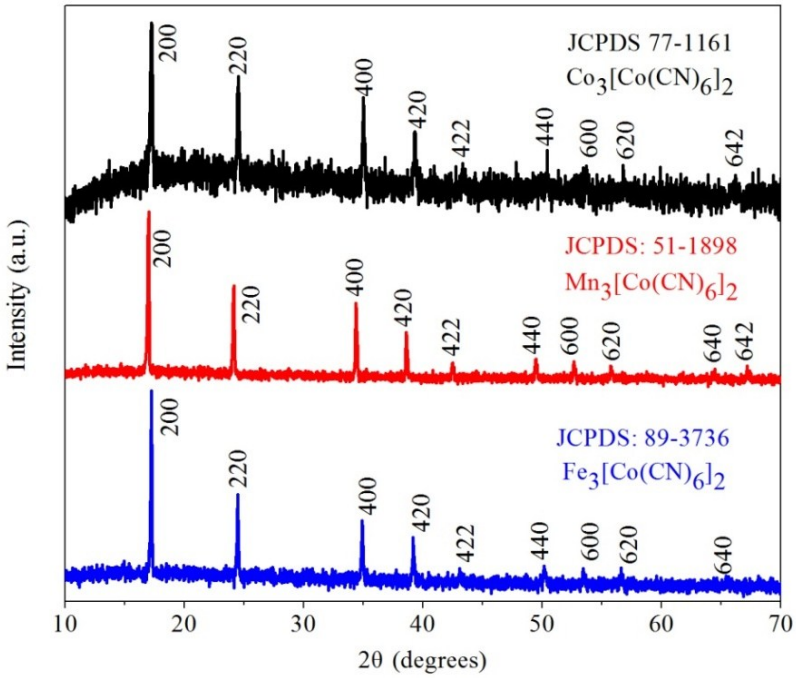

Figure S2. PXRD patterns of $Co_3[Co(CN)_6]_2$, $Mn_3[Co(CN)_6]_2$ and $Fe_3[Co(CN)_6]_2$ precursor nanocubes.

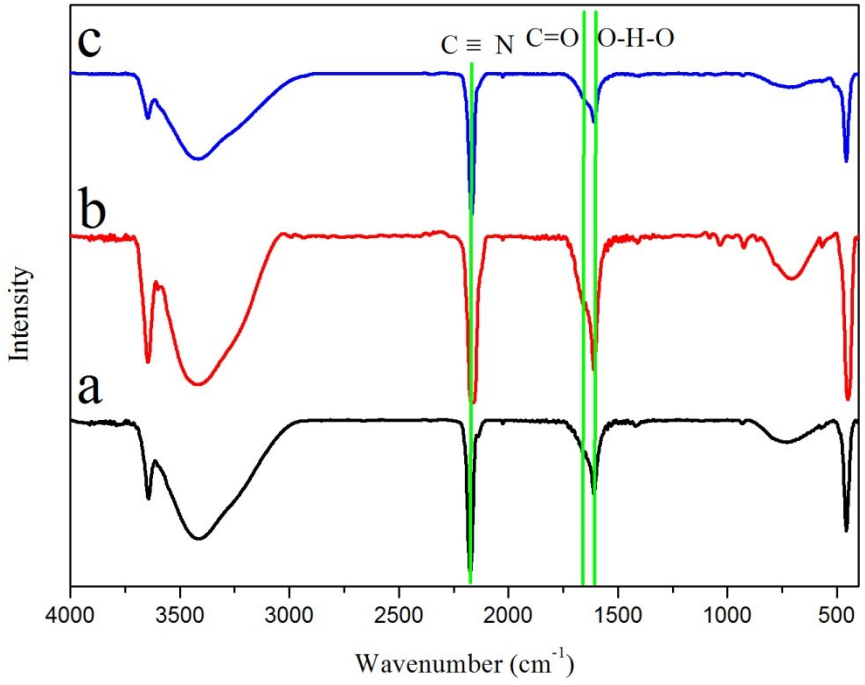

Figure S3. FTIR spectra of $Co_3[Co(CN)_6]_2$, $Mn_3[Co(CN)_6]_2$ and $Fe_3[Co(CN)_6]_2$ precursor nanocubes.

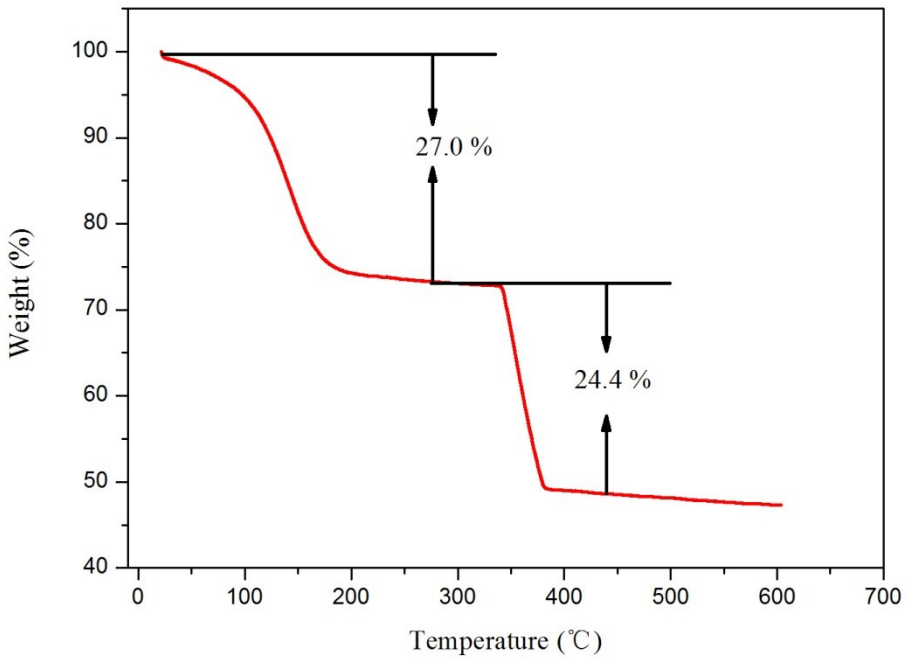

Figure S4. TGA curve of $Co_3[Co(CN)_6]_2 \cdot nH_2O$ precursor nanocubes in air flow with a ramp of 10 $^oC\ min^{-1}$.

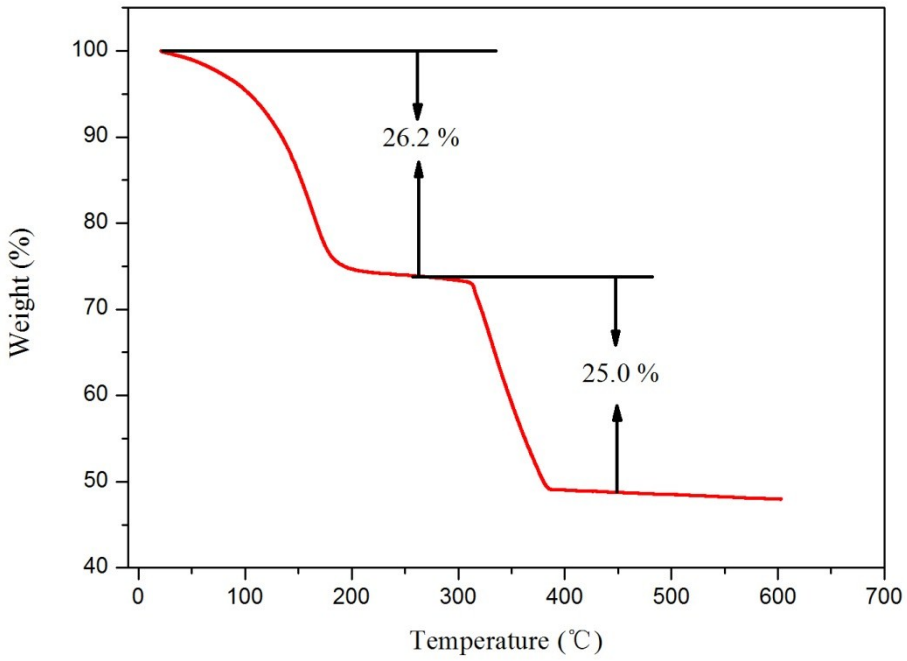

Figure S5. TGA curve of $Mn_3[Co(CN)_6]_2 \cdot nH_2O$ precursor nanocubes in air flow with a ramp of 10 $^oC\ min^{-1}$.

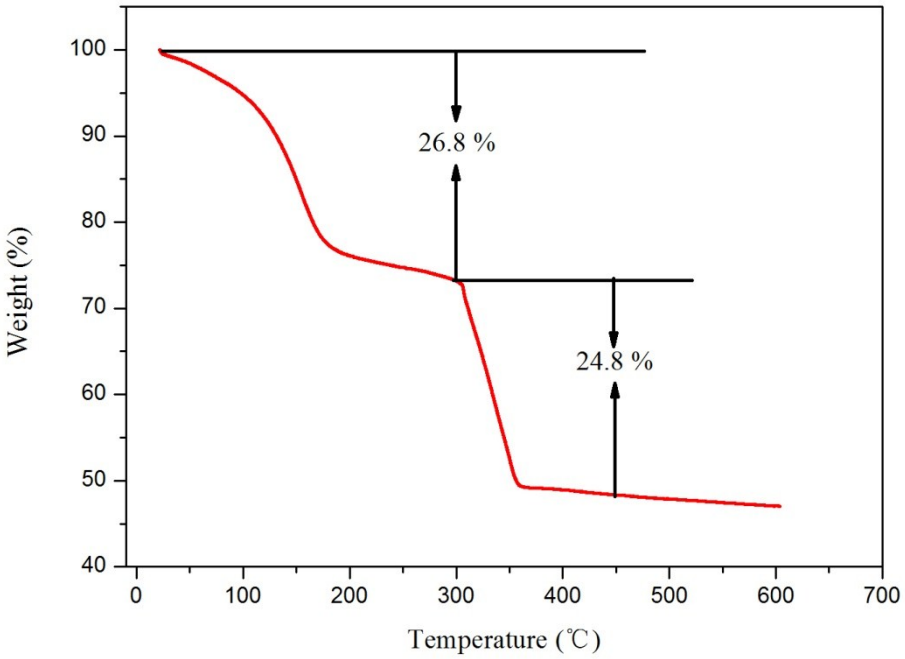

Figure S6. TGA curve of $Fe_3[Co(CN)_6]_2 \cdot nH_2O$ precursor nanocubes in air flow with a ramp of 10 $^oC\ min^{-1}$.

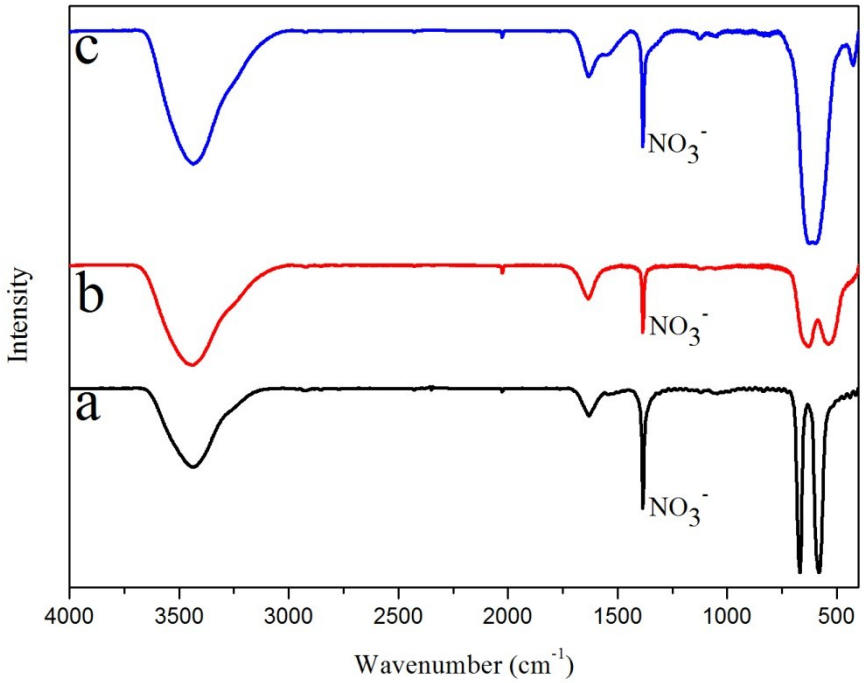

Figure S7. FTIR spectra of Co_3O_4 (a), $Mn_xCo_{3-x}O_4$ (b) and $Fe_xCo_{3-x}O_4$ (c) nanocubes.

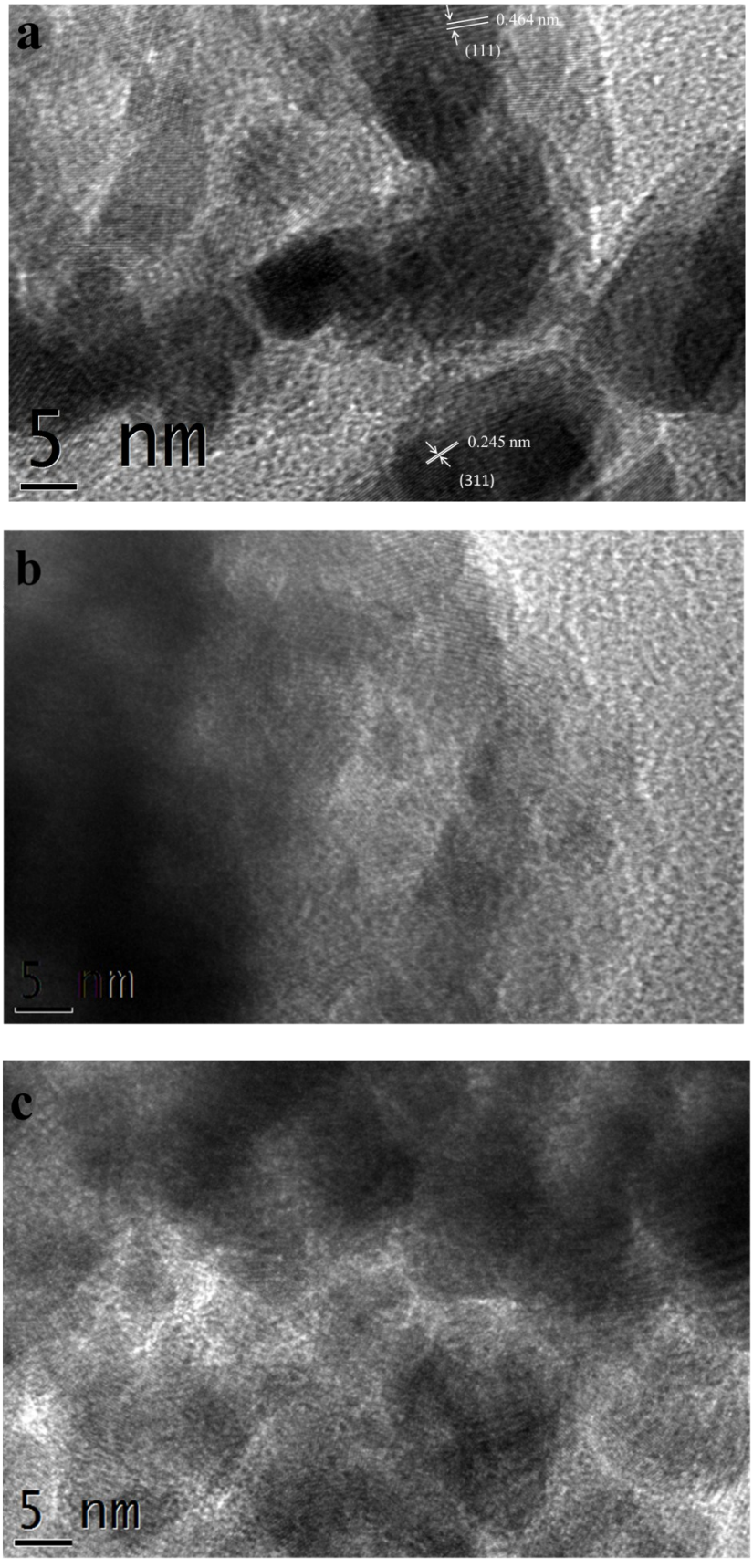

Figure S8. HRTEM images for as-prepared (a) Co_3O_4 nanocages, (b) $Mn_xCo_{3-x}O_4$ nanocages and (c) $Fe_xCo_{3-x}O_4$ nanocages.

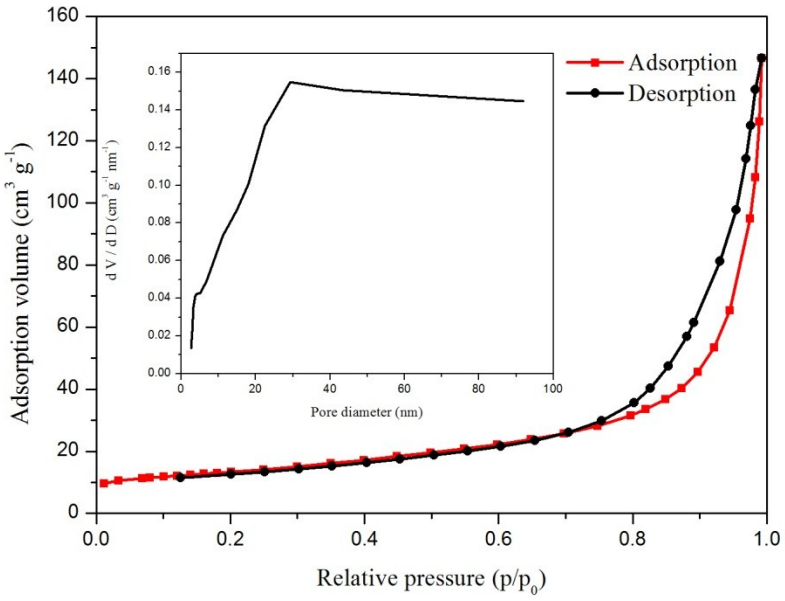

Figure S9. N_2 adsorption/desorption isotherm (77 K) curves for Co_3O_4 porous nanocages. Inset: The pore-size distribution of the Co_3O_4 nanocages.

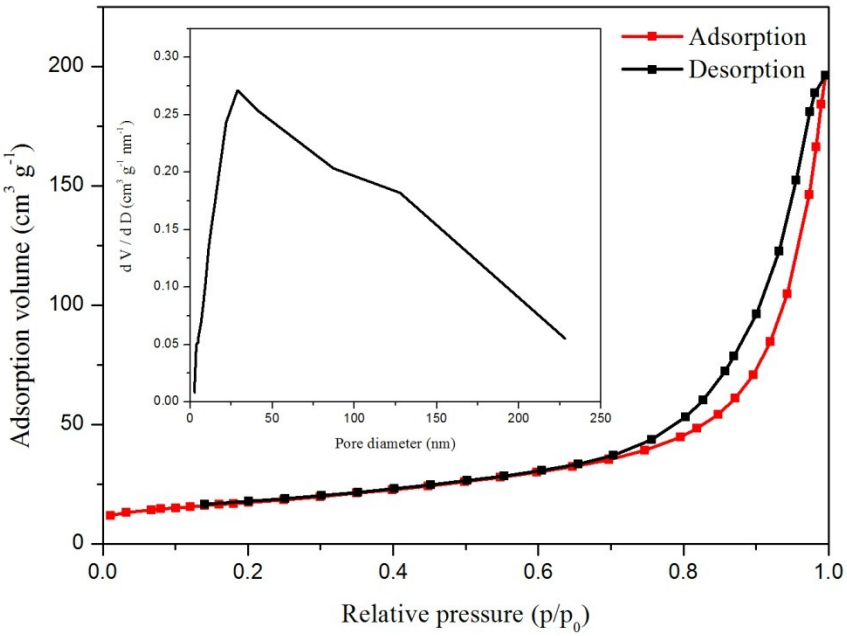

Figure S10. N_2 adsorption/desorption isotherm (77 K) curves for the $Mn_xCo_{3-x}O_4$ nanocages. Inset: The pore-size distribution of the $Mn_xCo_{3-x}O_4$ nanocages.

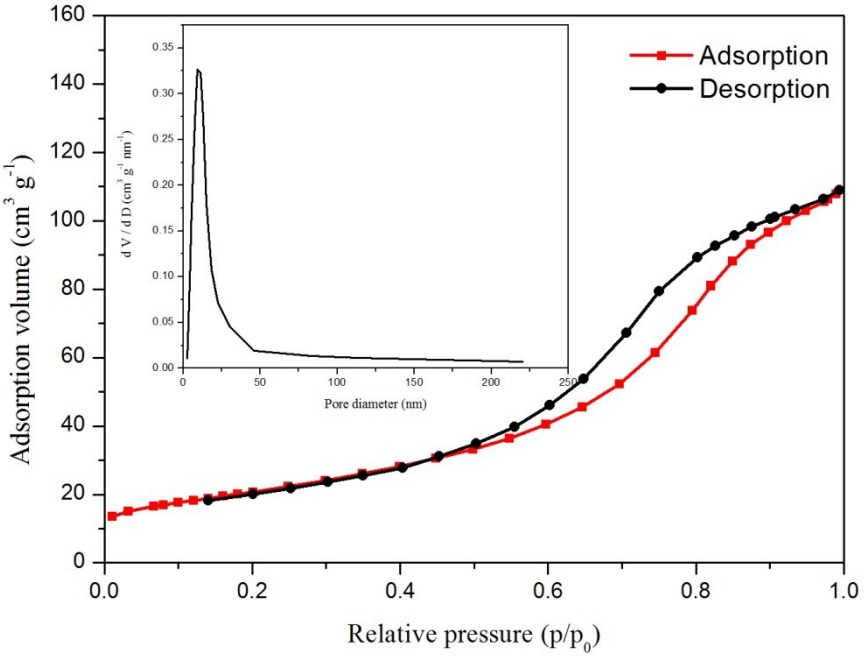

Figure S11. N_2 adsorption/desorption isotherm (77 K) curves for the $Fe_xCo_{3-x}O_4$ nanocages. Inset: The pore-size distribution of the $Fe_xCo_{3-x}O_4$ nanocages.

Table S1. Determination of metal elements ratio in porous nanocages oxides obtained by ICP-AES and EDX.

Catalyst	Estimated formula	Mn/Fe to Co ratio (Theo.)	Mn/Fe to Co ratio (EDX)	Mn/Fe to Co ratio (ICP-AES)
Co_3O_4	Co_3O_4	N/A	N/A	N/A
$Mn_xCo_{3-x}O_4$	$Mn_{1.8}Co_{1.2}O_4$	1.5:1	1.48:1	1.52:1
$Fe_xCo_{3-x}O_4$	$Fe_{1.8}Co_{1.2}O_4$	1.5:1	1.47:1	1.48:1

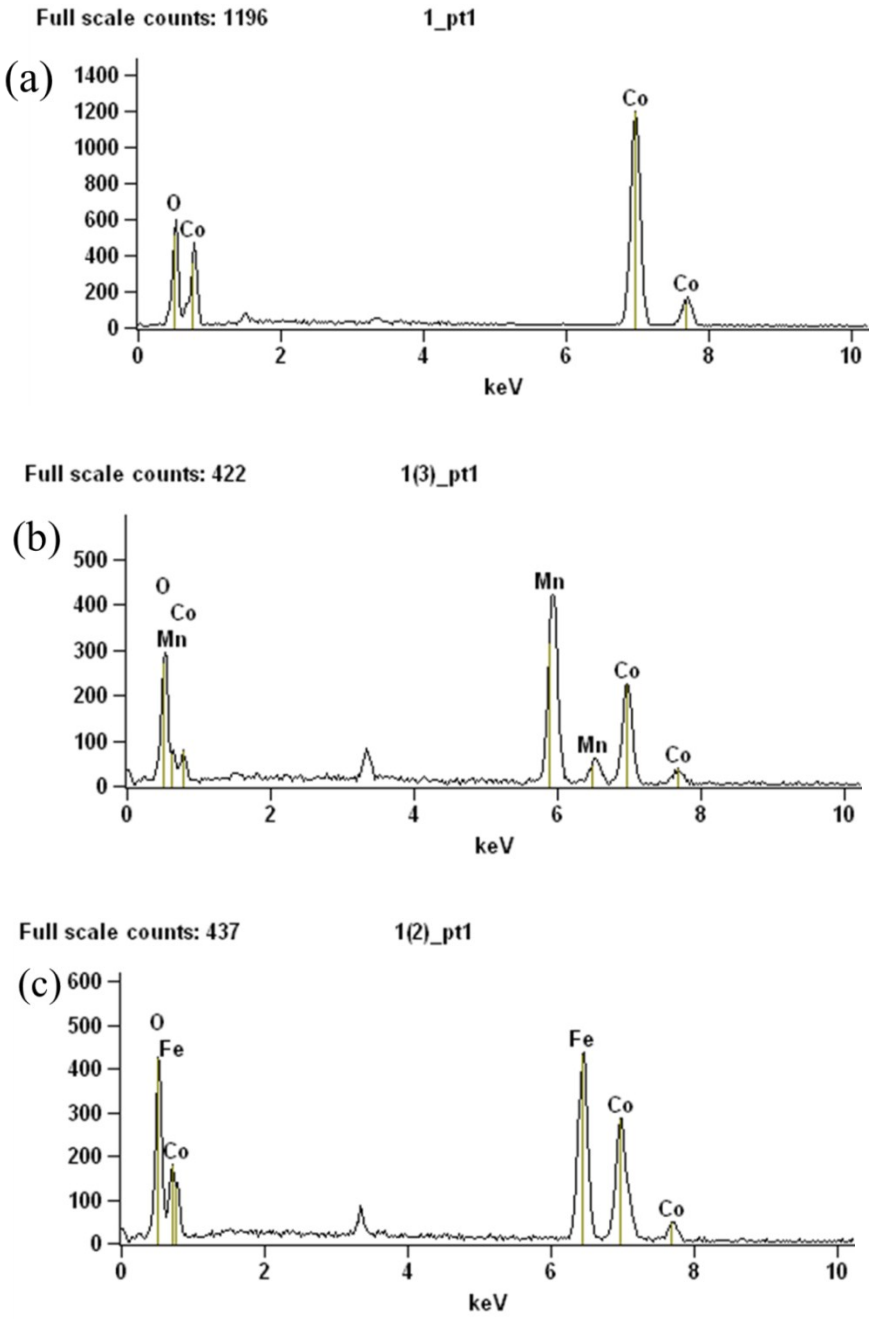

Figure S12. EDX measurements of Co, Mn and Fe in (a) Co_3O_4, (b) $Mn_xCo_{3-x}O_4$ and (c) $Fe_xCo_{3-x}O_4$.

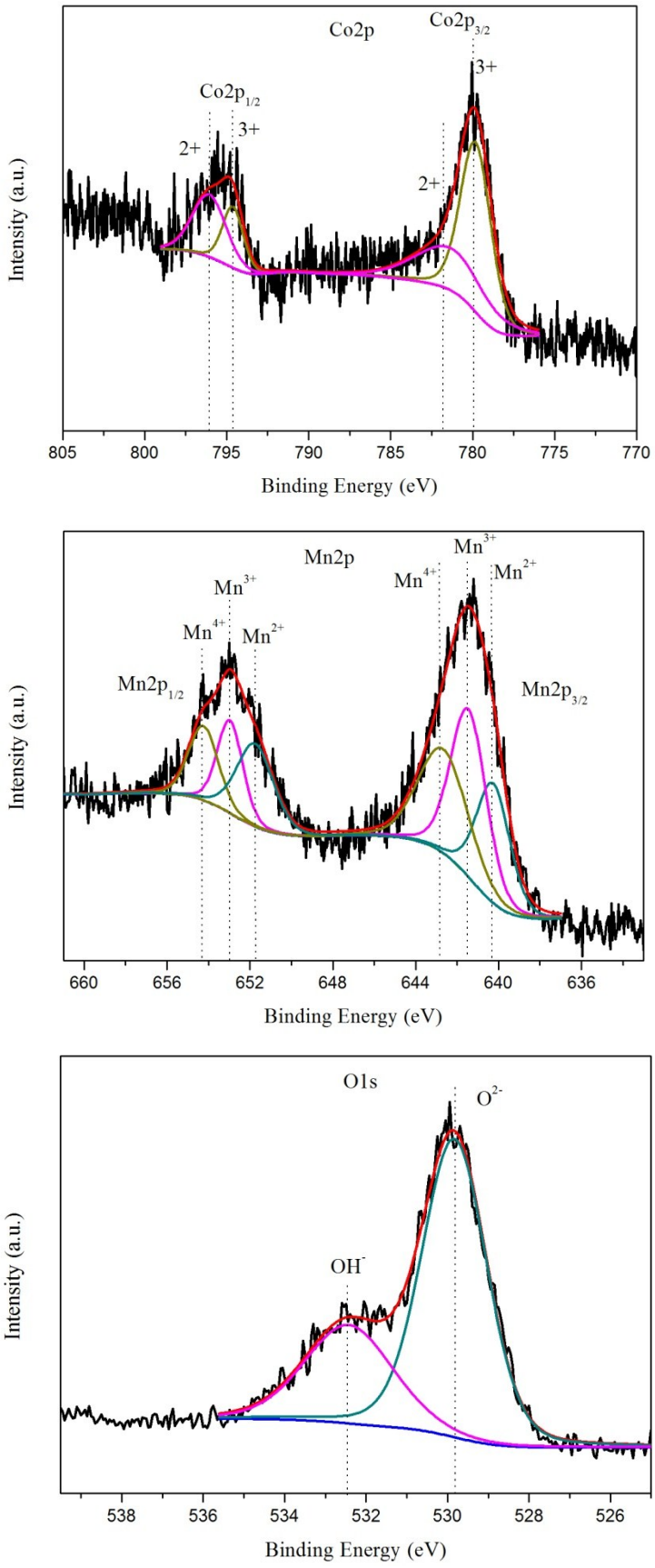

Figure S13. Co 2p (top), Mn 2p (middle) and O 1s (bottom) XPS spectra of $Mn_xCo_{3-x}O_4$ nanocages.

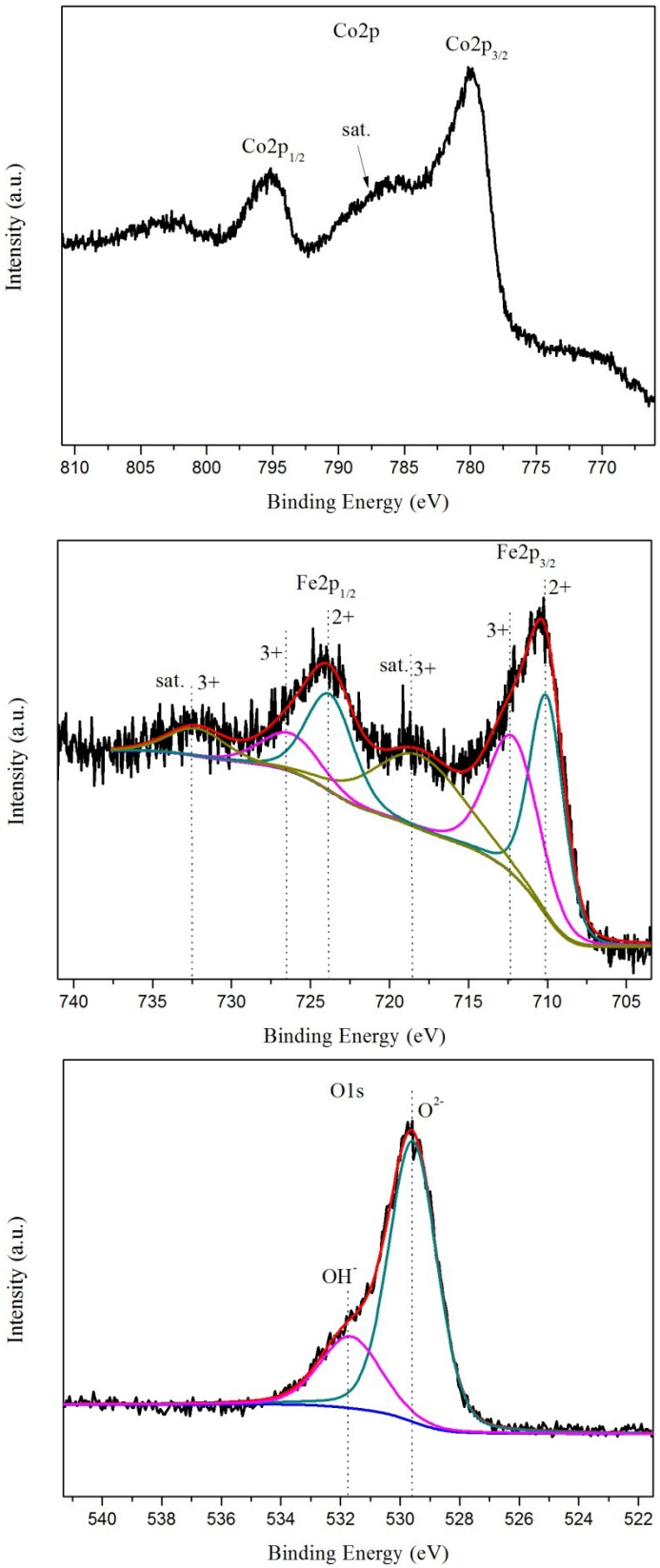

Figure S14. Co 2p (top), Fe 2p (middle) and O 1s (bottom) XPS spectra of $Fe_xCo_{3-x}O_4$ nanocages.

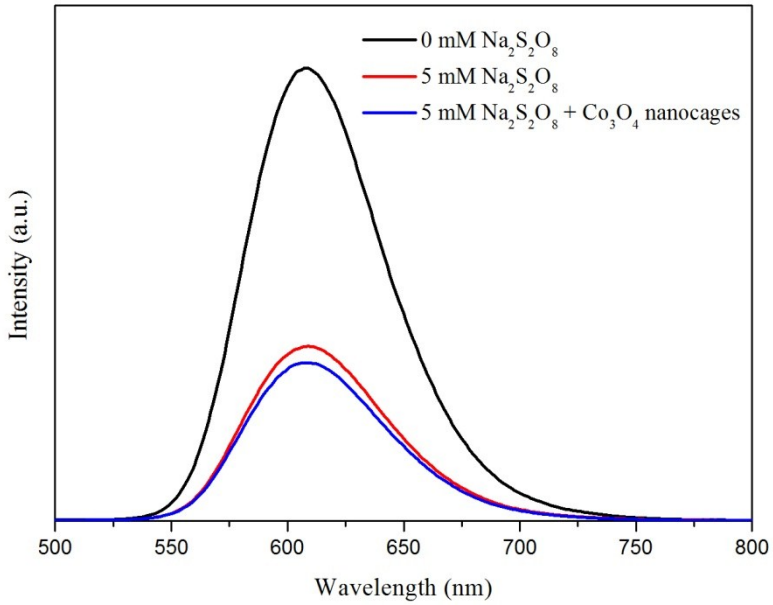

Figure S15. Steady-state luminescence spectra (λ_{ex} = 450 nm) of 1 mM $[Ru(bpy)_3]Cl_2$ in 100 mM phosphate buffer (pH 7.0) containing 5.0 mM persulfate or 0.2 g L^{-1} catalyst.

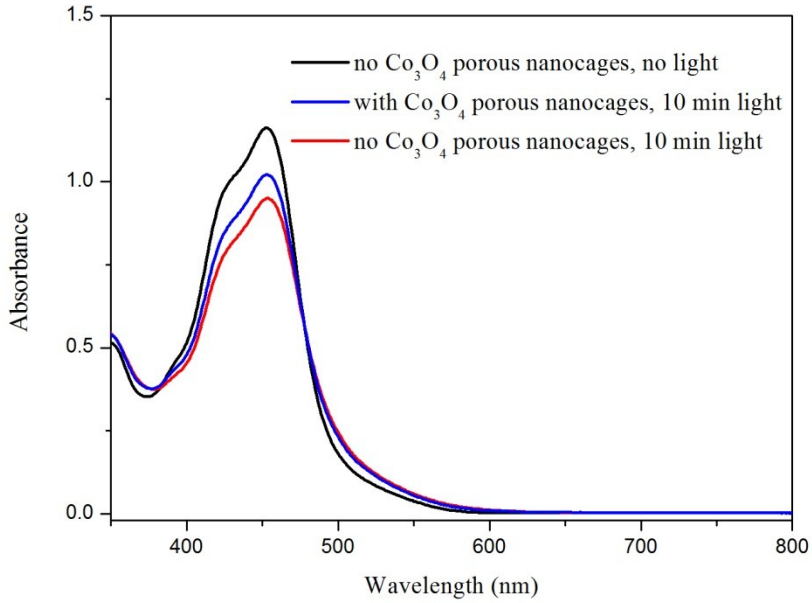

Figure S16. UV-vis spectral changes during the photocatalytic O_2 evolution with or without catalyst. (absorption of $[Ru(bpy)_3]Cl_2$ at 450 nm).

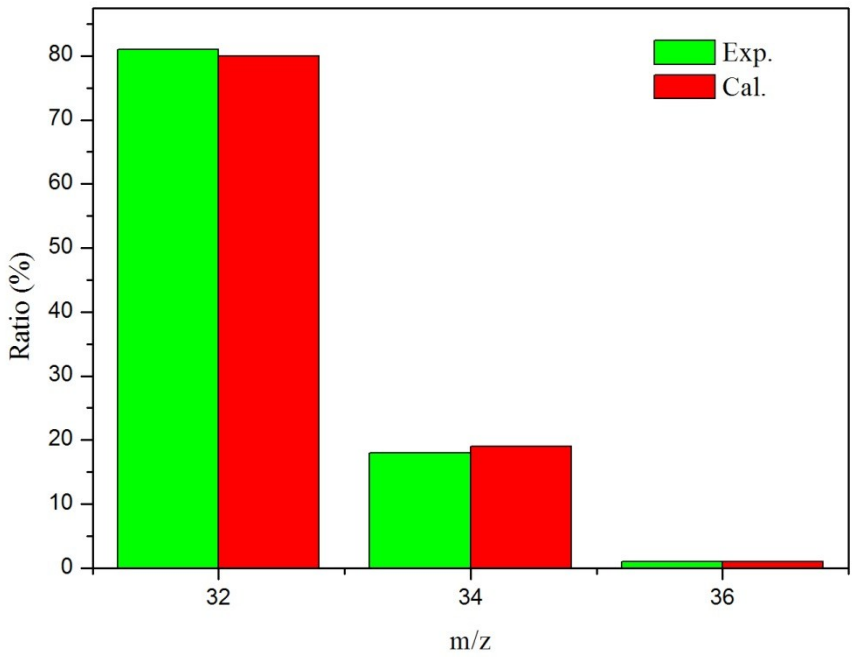

Figure S17. Observed and theoretical relative abundances of ^{18}O-labeled and unlabeled oxygen evolved during the photocatalytic oxidation of a buffer solution (4.5 mL) prepared with $H_2{}^{18}O$-enriched water (10.8% $H_2{}^{18}O$) containing Co_3O_4 porous nanocages (0.50 g L^{-1}), $[Ru(bpy)_3]Cl_2$ (1.0 mM) and $Na_2S_2O_8$ (5.0 mM) (green, observed mass intensity; red, calculated values assuming that evolved O_2 results exclusively from water).

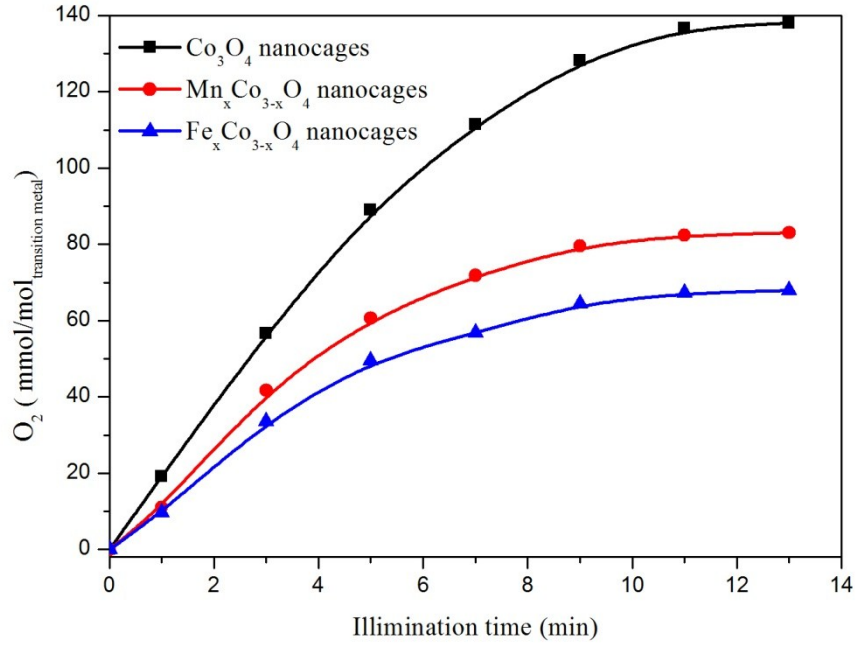

Figure S18. The per mole of transition metal normalized plot of photochemical water oxidation of a phosphate buffer solution (pH 7.0, 15.0 mL) containing $Na_2S_2O_8$ (5.0 mM), $[Ru(bpy)_3]Cl_2$ (1.0 mM) and catalyst (0.50 g L^{-1}) at room temperature.

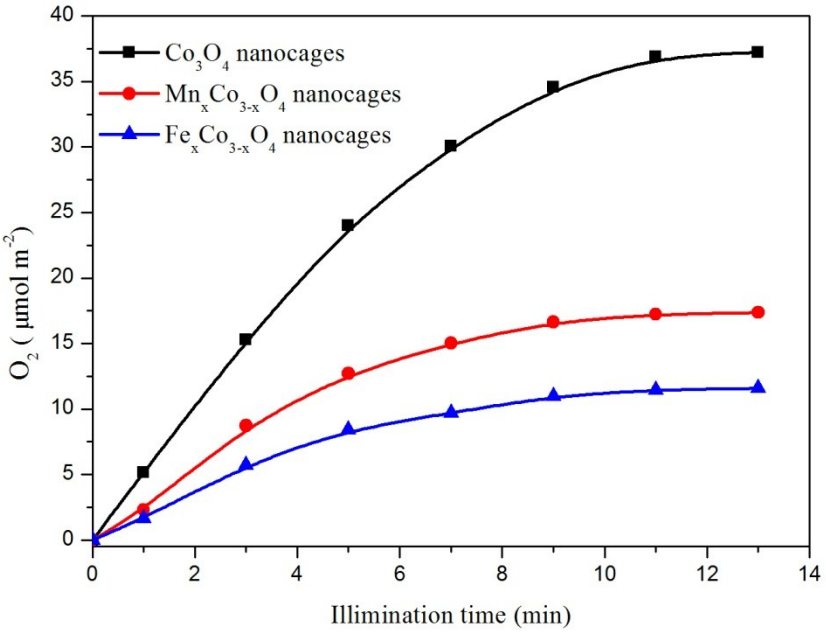

Figure S19. The surface-area normalized plot of photochemical water oxidation of a phosphate buffer solution (pH 7.0, 15.0 mL) containing $Na_2S_2O_8$ (5.0 mM), $[Ru(bpy)_3]Cl_2$ (1.0 mM) and catalyst (0.50 g L^{-1}) at room temperature.

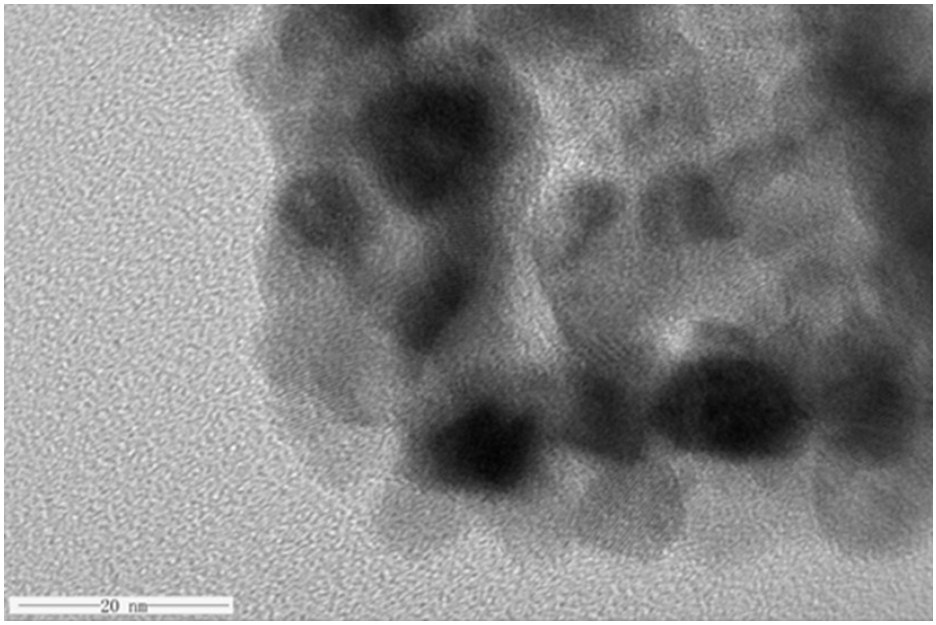

Figure S20. HRTEM images of Co_3O_4 porous nanocages after photocatalytic water oxidation.

Table S2. TOFs of some recently-reported Co-based heterogeneous water oxidation catalysts under visible light irradiation.

Catalyst	BET surface area (m^2/g)	Apparent TOF ($\mu mol\ s^{-1}\ m^{-2}$)[a]	TOF ($mol_{O2}\ mol_{metal}^{-1}\ s^{-1}$)	ref
Co_3O_4 nanocages	46.2	8.6×10^{-2}	3.2×10^{-4}	This work
$Mn_xCo_{3-x}O_4$ nanocages	61.4	3.8×10^{-2}	2.3×10^{-4}	This work
$Fe_xCo_{3-x}O_4$ nanocages	74.8	3.2×10^{-2}	1.9×10^{-4}	This work
Co_3O_4 supported in mesoporous silica	550-660	-	$2.12 \times 10^{-4} \sim 4.05 \times 10^{-4}$	1,2
Mesoporous Mg-Substituted Co_3O_4	102.1	-	2.4×10^{-4}	3
Hollow Co_3O_4	180	-	2.7×10^{-4}	4
Co_3O_4 micelle	12	-	1.45×10^{-3}	5
$MnCo_2O_4$	37	-	1.23×10^{-3}	6
$CoMn_2O_4$	11	-	5.3×10^{-4}	6
$LaCoO_3$	13	-	6.5×10^{-4}	7

[a]Apparent TOF= mole of oxygen produced in 1 min/(BET • 60 s)

Table S3. TOFs of some recently-reported Co-based heterogeneous water oxidation catalysts under cerium (IV)-driven condition.

Catalyst	BET surface area	Apparent TOF ($\mu mol\ s^{-1}\ m^{-2}$)	TOF ($mol_{O2}\ mol_{metal}^{-1}\ s^{-1}$)	ref
Co_3O_4 nanocages	46.2	0.96	3.6×10^{-3}	This work
$Mn_xCo_{3-x}O_4$ nanocages	61.4	8.9×10^{-2}	4.2×10^{-4}	This work
$Fe_xCo_{3-x}O_4$ nanocages	74.8	1.9×10^{-2}	1.1×10^{-4}	This work
Mesoporous Mg-Substituted Co_3O_4	102.1		2.2×10^{-4}	3
KIT-6/Co_3O_4			$3.4\text{-}5.3 \times 10^{-4}$	2
Co_3O_4 micelle	12	-	1.49×10^{-3}	5
$MnCo_2O_4$	37	-	3.5×10^{-4}	6
$CoMn_2O_4$	11	-	1.6×10^{-4}	6

Table S4. Summary of the electrochemical water oxidation activities of cobalt oxides.

Catalyst	overpotential (mV) at 0.5 mA cm^{-2}	overpotential (mV) at 1.0 mA cm^{-2}	pH	ref
Co_3O_4 porous nanocages	350	420	7	This work
Co_3O_4 nanoparticle (< 5 nm)	314	—	14	8
Co_3O_4 micelle	410	—	7	5
Co-P film	—	410	7	9

1. F. Jiao and H. Frei, *Angew. Chem. Int. Ed.*, 2009, **48**, 1841-1844.
2. S. Yusuf and F. Jiao, *ACS Catal.*, 2012, **2**, 2753-2760.
3. J. Rosen, G. S. Hutchings and F. Jiao, *J. Am. Chem. Soc.*, 2013, **135**, 4516-4521.
4. J. Zhao, Y. Zou, X. Zou, T. Bai, Y. Liu, R. Gao, D. Wang and G. D. Li, *Nanoscale*, 2014, **6**, 7255-7262.
5. P. W. Menezes, A. Indra, D. Gonzalez-Flores, N. R. Sahraie, I. Zaharieva, M. Schwarze, P. Strasser, H. Dau and M. Driess, *ACS Catal.*, 2015, **5**, 2017-2027.
6. P. W. Menezes, A. Indra, N. R. Sahraie, A. Bergmann, P. Strasser and M. Driess, *ChemSusChem*, 2015, **8**, 164-171.
7. Y. Yamada, K. Yano, D. Hong and S. Fukuzumi, *Phys. Chem. Chem. Phys.*, 2012, **14**, 5753-5760.
8. J. D. Blakemore, H. B. Gray, J. R. Winkler and A. M. Müller, *ACS Catal.*, 2013, **3**, 2497-2500.
9. M. W. Kanan and D. G. Nocera, *Science*, 2008, **321**, 1072-1075.